0.DC1.html

Mice fed a lipogenic methionine-choline-deficient diet develop hypermetabolism coincident with hepatic suppression of SCD-1[S]

Gizem Rizki,*,† Lorenzo Arnaboldi,[1],§ Bianca Gabrielli,§ Jim Yan,*,† Gene S. Lee,*,† Ray K. Ng,*,† Scott M. Turner,** Thomas M. Badger,†† Robert E. Pitas,§,§§ and Jacquelyn J. Maher[2],*,†

Departments of Medicine* and Pathology§§ and Liver Center,† University of California, San Francisco, San Francisco, CA; Gladstone Institute of Cardiovascular and Neurological Disease,§§ San Francisco, CA; KineMed,** Emeryville, CA; and Arkansas Children's Nutrition Center,†† University of Arkansas, Little Rock, AR

Abstract Lipogenic diets that are completely devoid of methionine and choline (MCD) induce hepatic steatosis. MCD feeding also provokes systemic weight loss, for unclear reasons. In this study, we found that MCD feeding causes profound hepatic suppression of the gene encoding stearoyl-coenzyme A desaturase-1 (SCD-1), an enzyme whose regulation has significant effects on metabolic rate. Within 7 days of MCD exposure, hepatic SCD-1 mRNA decreased to nearly undetectable levels. By day 21, SCD-1 protein was absent from hepatic microsomes and fatty acids showed a decrease in monounsaturated species. These changes in hepatic SCD-1 were accompanied by signs of hypermetabolism. Calorimetry revealed that MCD-fed mice consumed 37% more energy than control mice ($P = 0.0003$). MCD feeding also stimulated fatty acid oxidation, although fatty oxidation genes were not significantly upregulated. Interestingly, despite their increased metabolic rate, MCD-fed mice did not increase their food consumption, and as a result, they lost 26% of their body weight in 21 days. In summary, MCD feeding suppresses SCD-1 in the liver, which likely contributes to hypermetabolism and weight loss. MCD feeding also induces hepatic steatosis, by an independent mechanism. Viewed together, these two disparate consequences of MCD feeding (weight loss and hepatic steatosis) give the appearance of an unusual form of lipodystrophy.—Rizki, G., L. Arnaboldi, B. Gabrielli, J. Yan, G. S. Lee, R. K. Ng, S. M. Turner, T. M. Badger, R. E. Pitas, and J. J. Maher. Mice fed a lipogenic methionine-choline-deficient diet develop hypermetabolism coincident with hepatic suppression of SCD-1. *J. Lipid Res.* 2006. 47: 2280–2290.

Elimination of methionine and choline from the diet causes fat to accumulate rapidly within the liver (1). In this situation, steatosis is the result of impaired hepatic tri-

glyceride secretion, which in turn is attributable to defective assembly of VLDL (2). Methionine and choline are important precursors of phosphatidylcholine, the principal phospholipid comprising the outer coat of VLDL particles (3). When these nutrients are in short supply, VLDL production is impaired and triglycerides accumulate in hepatocytes (2, 4). When a lipogenic substrate such as sucrose is incorporated into a dietary formula that lacks methionine and choline, its ability to provoke hepatic steatosis is accentuated. Lipogenic methionine-choline-deficient (MCD) formulas induce not only steatosis but also hepatic inflammation and fibrosis (1, 5, 6). This severe and progressive liver injury distinguishes the MCD model of fatty liver from others in which inflammation and fibrosis are rare (7–10).

Hepatic triglyceride secretion can be blocked by other means, such as knocking out the gene encoding microsomal triglyceride transfer protein (MTP) in a liver-specific manner. MTP is a peptide that facilitates the incorporation of triglycerides into VLDL (11); mice that lack this protein in the liver develop hepatic steatosis. In liver-specific MTP-deficient mice, fatty liver is associated with downregulation of the enzyme stearoyl-coenzyme A desaturase-1 (SCD-1) (12). SCD-1 catalyzes the conversion of two long-chain fatty acids, palmitate (C16:0) and stearate (C18:0), into their monounsaturated derivatives pal-

mitoleate (C16:1) and oleate (C18:1) (13). This desaturation step is critical for the incorporation of newly synthesized fatty acids into triglycerides (14). Mice that completely lack SCD-1 have a reduced capacity for fatty acid esterification into triglyceride (14). Conversely, they exhibit enhanced fatty acid catabolism via β-oxidation (15). The absence of SCD-1 promotes increased energy expenditure and a lean body habitus despite increased food consumption (15).

The potential link between inhibition of hepatic triglyceride secretion, suppression of SCD-1, and hypermetabolism is intriguing, because MCD-mediated blockade of hepatic triglyceride secretion causes weight loss (1). Based on the mechanistic similarity between MCD feeding and MTP deficiency, we hypothesized that MCD feeding would suppress SCD-1. In addition, based on reports of enhanced fatty acid oxidation in SCD-1-deficient mice, we reasoned that MCD-mediated suppression of SCD-1 would stimulate fatty acid oxidation and increase oxygen consumption. MCD feeding did indeed downregulate SCD-1 and increase fatty acid flux through the β-oxidation pathway. This resulted in a marked increase in energy expenditure, which ultimately resulted in weight loss.

METHODS

MCD feeding

Male C3H/HeOuJ mice (Jackson Laboratory, Bar Harbor, ME) weighing 23–28 g were used for all studies. Animals were divided into three groups, each of which received a different dietary formula for a period of 21 days. One group of mice was fed a high-sucrose, high-fat diet completely devoid of methionine and choline (MCD) (No. 960439; ICN Biomedicals, Irvine, CA). The MCD formula comprised 17% protein (as defined amino acids), 65% carbohydrate (70:30 sucrose-starch), and 10% fat (as corn oil). The second group of mice was fed a control formula identical to the MCD formula except that it was supplemented with 3 g/kg DL-methionine and 2 g/kg choline chloride [methionine-choline-sufficient (MCS)] (No. 960441; ICN Biomedicals). The third group of mice was fed standard rodent chow (Laboratory Rodent Diet 5001; LabDiet, Richmond, IN). The chow diet comprised 23% protein, 56% carbohydrate, and 4.5% fat. While eating the experimental formulas, all animals had free access to drinking water. On the final day of the experiment, mice were fasted for 4 h before euthanasia.

At the time of death, blood was collected from the thoracic aorta. Serum was separated from cellular elements by centrifugation. Livers were removed, rinsed in ice-cold saline solution, and divided for various assays as outlined below. All experimental protocols were approved by the Committee on Animal Research at the University of California, San Francisco.

Serum chemistries

Serum glucose and alanine aminotransferase were measured on a BAX autoanalyzer (Bayer Corp., Tokyo, Japan). Leptin and insulin were measured by ELISA [Quantikine rat/mouse leptin assay kit (R&D Systems, Minneapolis, MN); mouse insulin ELISA (Linco, St. Charles, MO)]. Serum cholesterol, triglycerides, and β-hydroxybutyrate were assayed enzymatically using colorimetric kits (Boehringer Mannheim GmbH Diagnostica, Montreal, Canada; Stanbio Laboratory, Boerne, TX).

Measurement of hepatic gene expression by real-time quantitative PCR

Total RNA was extracted from mouse liver by homogenization in TRI reagent (Molecular Research Center, Cincinnati, OH) followed by chloroform extraction and ethanol precipitation. RNA was incubated with DNase (Qiagen, Inc., Valencia, CA) to remove contaminating DNA; the enzyme was then inactivated and removed according to the manufacturer's specifications (RNeasy; Qiagen). cDNA was synthesized from 1 μg of RNA in a reaction mixture containing 2.5 U/μl Moloney murine leukemia virus reverse transcriptase (Invitrogen, Carlsbad, CA) and 5 μM random hexamer primers (No. 48190-011; Invitrogen). Real-time PCR analysis was performed using an ABI Prism 7900 sequence detection system (Applied Biosystems, Foster City, CA). Assays-on-Demand® (Applied Biosystems) were used to measure all genes except SCD-1 and acetyl-coenzyme A carboxylase (ACC). For these, primers and probes were designed using Primer Express software (version 1.5; Applied Biosystems) (see supplementary Table I). Gene expression was assayed in triplicate by real-time PCR using a master mix of 5.5 mM $MgCl_2$, 200 μM deoxynucleoside triphosphates, and 0.5 units of Amplitaq Gold® (Applied Biosystems). Primer and probe concentrations were 500 and 200 nM, respectively, and cDNA was added in an amount equivalent to 3–5 ng of input RNA. The expression of each test gene was normalized to that of mouse β-glucuronidase. Quantitative detection of specific nucleotide sequences was based on the fluorogenic 5′ nuclease assay (16). Relative gene expression was calculated using the method of Livak and Schmittgen (17).

Extraction and analysis of hepatic lipids

Samples of fresh liver tissue weighing 100–200 mg were homogenized in 2 ml of ice-cold methanol containing 0.01% (w/v) butylated hydroxytoluene (BHT). Homogenates were supplemented with 4 ml of chloroform containing 0.01% BHT, and KCl was added to a final concentration of 50 mM. The solutions were mixed by vigorous vortexing; they were then centrifuged at 850 g for 10 min. Organic layers were transferred to fresh test tubes. Aqueous layers were reextracted with chloroform/BHT; the second organic extract from each liver was then pooled with the first, and the entire sample was dried under a continuous stream of nitrogen gas. Dried lipid extracts were resuspended in 2:1 chloroform-methanol containing 0.01% BHT (500 μl/100 mg liver weight). Samples were stored in light-shielded glass containers at −80°C.

For measurement of total liver cholesterol, aliquots of hepatic lipid extract were suspended in 1% Triton X-100 and heated to 50°C before assaying with a commercial kit (Boehringer Mannheim). Total hepatic phospholipid was determined by hydrolyzing lipid extracts and K_2HPO_4 standards in 0.3 ml of 1 N H_2SO_4 at 150°C overnight and decolorizing with hydrogen peroxide (5% final concentration). Samples and standards were then supplemented with 0.3 ml of water, 0.1 ml of ascorbic acid (0.1 g/ml), and 0.6 ml of ammonium molybdate in 1 N H_2SO_4 (0.01 g/ml). The mixtures were incubated at 55°C for 20 min and then assayed for color development at 750 nm. Total hepatic triglyceride was measured chromatographically as described below. Cholesterol and triglyceride concentrations were expressed in μg/g liver. Phospholipid concentrations were expressed as nmol phosphorus/g liver.

FFAs, cholesteryl esters, and triglycerides were separated from crude hepatic lipid extracts by thin-layer chromatography using a solvent system of hexane-diethyl ether-acetic acid (80:20:1).

Bands corresponding to individual lipid fractions were identified with dichlorofluorescein and verified against known standards (Nonpolar Lipid Mix B; Matreya, Pleasant Gap, PA). Bands containing triglycerides were scraped from the TLC plate into separate glass tubes; a known amount of triheptadecanoin was added as an internal standard, and fatty acid methyl esters were generated by incubation with 3 N methanolic HCl/toluene (4:1) for 2 h at $37°C$. The methyl esters were then extracted with hexane-water and analyzed by gas chromatography (HP Chem Station 6890 Series; Hewlett-Packard, Palo Alto, CA) on a fused silica capillary column, with polyethylene glycol as the stationary phase (Alltech ECTM^{WAX} 30 m, 0.25 mm inner diameter, 0.25 μm film). The relative proportion of individual fatty acids in each lipid subclass was obtained by integrating the peaks using the HP Chem Station Standard Integrator Algorithm (Hewlett-Packard). The total amount of fatty acid in the triglyceride fraction was calculated by analyzing peak area in comparison with the internal standard. Similar methods were used to determine the fatty acid composition of hepatic FFAs (18). FFA analysis was performed by Lipomics Technologies (West Sacramento, CA).

Preparation of hepatic microsomes

Fresh liver tissue weighing 100–200 mg was homogenized with a motorized Teflon pestle in 5 volumes of ice-cold 0.25 M sucrose, 50 mM HEPES (pH 7.4), 5 mM DTT, and 1× protease inhibitor cocktail (Halt™; Pierce Biotechnology). Crude homogenates were pelleted by centrifugation at 22,000 g for 10 min, and the supernatants were subjected to a second round of centrifugation at 150,000 g for 40 min. Microsomal pellets were suspended in 20% glycerol, 5 mM HEPES (pH 7.4), 5 mM DTT, and 1× protease inhibitor cocktail. Protein concentration was measured by the Bradford assay (Bio-Rad, Hercules, CA), and the remainder of each sample was stored in aliquots at $-80°C$.

Western blotting

Antibodies directed against AMP-activated protein kinase (AMPK) and phosphorylated AMPK (threonine 172) were obtained from Cell Signaling Technology (Beverly, MA). Rabbit anti-rat SCD-1 antibody was a gift from Dr. Juris Ozols (University of Connecticut) (19). Liver homogenates or hepatic microsomal extracts were separated by electrophoresis through SDS-polyacrylamide and transferred to polyvinylidene difluoride membranes. The membranes were blocked for 1 h at room temperature in Tris-buffered saline containing 5% (w/v) nonfat dry milk and 0.1% Tween-20. After overnight incubation at $4°C$ with primary antibody, the membranes were washed three times and incubated for 1 h with peroxidase-conjugated goat anti-rabbit IgG (1:10,000; Cell Signaling Technology). Immunoreactive proteins were detected by chemiluminescence (SuperSignal® West Dura; Pierce Chemical Co.).

De novo lipogenesis

De novo lipogenesis (DNL) was measured by mass isotopomer distribution analysis as described (20–22). Three days before euthanasia, mice were injected with 0.9% NaCl prepared with ^2H_2O (30 ml/kg ip) and maintained at steady state by administration of drinking water containing 8% ^2H_2O. Triglycerides were extracted from whole liver as described by Jung and colleagues (23) and derivatized for analysis by GC-MS (Agilent Corp., Palo Alto, CA). For methyl palmitate, the molecular anion and its isotopes (m/z 270–272, representing M_0–M_2) were quantified under the selected ion monitoring mode. Calculations were based on 22 possible sites for deuterium incorporation (24, 25).

Palmitate oxidation and carnitine palmitoyltransferase activity

Hepatic mitochondria were prepared as described (26), except that the buffer used for the initial tissue homogenization step was supplemented with 2% BSA. Palmitate oxidation was measured by adding 200 μl of fresh mitochondrial suspension, corresponding to 250 μg of protein, to 380 μl of a reaction mixture containing 100 mM sucrose, 10 mM Tris-HCl, 0.2 mM EDTA, 5 mM KH_2PO_4, 80 mM KCl, 1 mM $MgCl_2$, 2 mM L-carnitine, 0.1 mM malate, 2 mM ATP, 0.05 mM CoA, 1 mM DTT, 0.3% fatty acid-free BSA, and 0.4 μCi of [^{14}C]palmitate (GE Life Sciences, Piscataway, NY). Incubations were performed for 30 min at $30°C$ in screw-capped vials fitted with Teflon sample seals and an internal well for trapping evolved CO_2. Reactions were stopped by injecting 200 μl of perchloric acid through the Teflon seal into the reaction mixture and gently mixing with a finger tap. A total of 200 μl of 1 N NaOH was then injected through the seal into the internal well to capture CO_2 from the atmosphere. One hour after the reaction was stopped, the vials were opened and the reaction mixture and NaOH were removed separately. The reaction mixture was clarified by centrifugation at 10,000 g. Radioactivity was counted in the supernatant and reported as acid-soluble intermediates. Radioactivity trapped in the NaOH fraction was reported as evolved CO_2. All radioactivity measurements were normalized to mitochondrial protein.

Carnitine palmitoyltransferase-1 (CPT-1) activity was measured in hepatic mitochondria by the method of Esser and colleagues (27) using [^{3}H]carnitine (GE Life Sciences) as a substrate. Enzyme activity was expressed as the amount of palmitoylcarnitine produced in an 8 min reaction, normalized to mitochondrial protein.

Indirect calorimetry

Oxygen consumption and carbon dioxide production were measured in an open-flow indirect calorimeter (Columbus Instruments, Columbus, OH) as described previously (28). Food intake and physical activity were measured simultaneously. Data were collected from three independent experiments, each involving three mice per diet group.

Statistical analysis

All experiments included at least five mice per study group. Mean data from each study group were compared by ANOVA. $P < 0.05$ was considered statistically significant.

RESULTS

Depriving mice of methionine and choline for 21 days caused a marked reduction in hepatic phospholipid content (**Table 1**). This was accompanied by a significant decrease in the concentration of serum triglyceride, which was presumably attributable to a phospholipid-related defect in hepatic triglyceride secretion. Low serum triglyceride levels in MCD-fed mice were accompanied by reciprocally high concentrations of hepatic triglyceride; liver weight-body weight ratios were also high in MCD-fed mice, indicative of steatosis. Liver histology confirmed marked fat accumulation and demonstrated focal inflammatory infiltrates (**Fig. 1**). This coincided with a significant increase in serum alanine aminotransferase (Table 1). As has been reported previously, MCD feeding provoked significant

TABLE 1. Clinical characteristics of mice after 21 days on experimental diets

Characteristic	Dietary Group		
	Chow	MCS	MCD
Body weight (g)	30.2 ± 0.8	38.2 ± 0.4^a	$19.6 \pm 0.2^{b,c}$
Liver weight (g)	1.39 ± 0.03	1.71 ± 0.03^a	$0.98 \pm 0.03^{b,c}$
Adipose weight (g)	1.5 ± 0.2	4.9 ± 0.2^a	$0.3 \pm 0.1^{b,c}$
Liver weight-body weight (%)	4.8 ± 0.1	4.6 ± 0.0	$5.1 \pm 0.1^{b,c}$
Adipose weight-body weight (%)	4.9 ± 0.4	13.1 ± 0.6^a	$1.61 \pm 0.4^{b,c}$
Serum triglyceride (mg/dl)	120.5 ± 27.8	122.9 ± 32.8	$46.4 \pm 3.4^{b,c}$
Serum cholesterol (mg/dl)	104.5 ± 3.3	145.5 ± 6.7^a	$77.2 \pm 6.2^{b,c}$
Serum alanine aminotransferase (IU/l)	79.75 ± 1.65	82.0 ± 2.7	$320.4 \pm 57.9^{b,c}$
Serum glucose (mg/dl)	245.2 ± 11.6	219.2 ± 21.0	$148.8 \pm 10.8^{b,c}$
Serum insulin (ng/ml)	0.87 ± 0.33	1.02 ± 0.14	0.41 ± 0.09^c
Serum leptin (ng/ml)	ND	13.9 ± 1.2	0.6 ± 0.1^c
Serum β-hydroxybutyrate (mg/dl)	3.3 ± 0.4	5.1 ± 1.1	$10.6 \pm 1.2^{b,c}$
Hepatic phospholipid (nmol/mg protein)	379.2 ± 10.4	434.5 ± 14.6	$363.4 \pm 14.9^{b,c}$
Hepatic triglyceride (µg/mg protein)	21.2 ± 2.3	136.6 ± 23.5^a	$815.8 \pm 60.2^{b,c}$
Hepatic cholesterol (µg/mg protein)	24.5 ± 0.8	31.0 ± 1.3	$21.8 \pm 3.6^{b,c}$

MCD, high-sucrose diet devoid of methionine and choline; MCS, high-sucrose diet supplemented with methionine and choline; ND, not determined. Values represent means $\pm$ SEM for n = 5.

[a] $P < 0.05$ for MCS versus chow.
[b] $P < 0.05$ for MCD versus chow.
[c] $P < 0.05$ for MCD versus MCS.

weight loss (1). Adipose tissue mass was markedly decreased in MCD-fed mice compared with controls, and serum leptin was also decreased to nearly undetectable levels. This combination of hepatic steatosis and weight loss is reminiscent of lipodystrophy, but MCD-fed mice lacked any evidence of insulin resistance, which is a characteristic feature of lipodystrophy syndromes (29).

Examination of liver-specific gene expression in mice fed the MCD formula for 21 days revealed significant alterations in several genes related to fatty acid and triglyceride synthesis (**Fig. 2A**). Lipogenic genes were expressed at much lower levels in MCD-fed mice than in MCS-fed controls; this was true even though both formulas were equally enriched in sucrose. In general, the lipogenic gene profile of MCD-fed mice resembled that of chow-fed mice, with two notable exceptions. MCD feeding suppressed sterol-regulatory element binding protein-1 (SREBP-1) and SCD-1 mRNA levels far below even the chow-fed baseline. SCD-1 mRNA in particular was reduced by 98%, to nearly undetectable levels. Downregulation of SCD-1 mRNA coincided with the disappearance of SCD-1 protein from hepatic microsomes (Fig. 2B).

Investigation of the kinetics of SCD-1 gene regulation revealed that MCD feeding initially induced SCD-1 mRNA expression in the liver (Fig. 2C). SCD-1 mRNA increased by 4-fold during the first 24 h of MCD feeding; immediately thereafter, it began to decline, decreasing to less than normal by day 4. By contrast, MCS feeding caused an 8-fold increase in SCD-1 mRNA at 24 h that was sustained for 21 days. In MCD-fed mice, the disappearance of SCD-1 mRNA exhibited first-order kinetics (Fig. 2D) with a predicted half-life of 45 h. This suggests that SCD-1 gene transcription ceased very soon after the introduction of the MCD formula.

To assess the impact of these diet-induced changes in gene expression on hepatic lipid metabolism, we measured DNL in the livers of mice fed MCD and control formulas for 21 days. As expected, both fractional and absolute DNL were greatest in mice fed the sucrose-rich MCS control formula (**Table 2**). In chow-fed controls, fractional DNL was high but absolute DNL was not; this reflected the low hepatic lipid content of chow-fed animals. In MCD mice, fractional DNL was quite low. This was likely attributable to the large pool of unlabeled lipid that had already accumulated in MCD livers before the introduction of the metabolic tracer. Absolute DNL in MCD-fed mice was intermediate between chow-fed and MCS controls, indicating that these mice retained some capacity for palmitate synthesis as predicted by their expression of ATP citrate lyase, acyl-CoA carboxylase, and fatty acid synthase (Fig. 2A).

MCD feeding altered the fatty acid composition of hepatic lipids in a manner commensurate with low SCD-1 activity. Specifically, MCD feeding provoked a 2- to 3-fold increase in the ratio of saturated to monounsaturated long-chain fatty acids in the liver in the triglyceride fraction (**Table 3**) as well as in hepatic free fatty acids (data not shown). Reduced desaturase activity was also reflected in the absolute amounts of saturated and monounsaturated long-chain fatty acids in the livers of MCD mice. In MCD-fed livers, saturated long-chain fatty acids exceeded monounsaturated fatty acids by 30%, whereas in chow-fed and MCS livers, the two species were equivalent (**Fig. 3**).

The diet-induced suppression of SCD-1 in MCD-fed mice was accompanied by evidence of hypermetabolism. After only 8 days of MCD feeding, MCD mice displayed a 37% increase in energy expenditure relative to MCS controls ($P = 0.0003$) (**Fig. 4A**). MCD-fed mice were not hyperthermic (MCD, $37.6 \pm 0.3°C$; MCS, $37.9 \pm 0.3°C$); they did, however, display a tendency to be more active than MCS-fed mice during nocturnal periods (25% increase) (Fig. 4B). MCD-fed mice also consumed nearly four times as much water as MCS controls ($P = 0.001$)
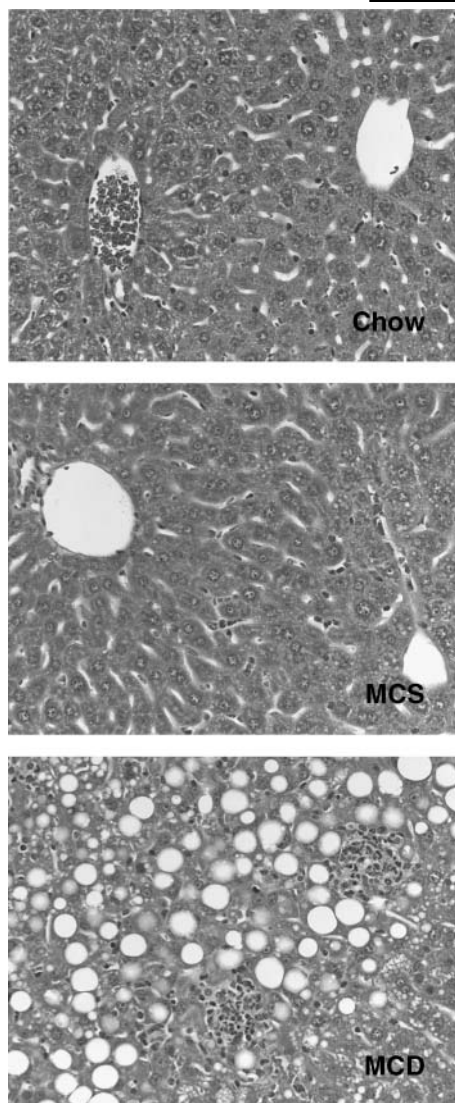
Fig. 1. Liver histology and serum alanine aminotransferase in mice fed methionine-choline-deficient (MCD) or control formulas. Photomicrographs show hematoxylin and eosin-stained sections of liver tissue from mice fed standard chow, the methionine-choline-sufficient (MCS) formula, or the MCD formula for 21 days. Histology in the chow and MCS livers appears normal. The MCD liver shows marked steatosis with focal aggregates of inflammatory cells.

(Fig. 4C), despite normoglycemia (Table 1). Notably, MCD-fed mice did not consume any more food than control mice (Fig. 4D). As a result, they lost a significant amount of weight over 21 days (Fig. 4E).

In scd-$1^{-/-}$ mice, hypermetabolism has been attributed to enhanced β-oxidation of fatty acids (15). In these mice, fatty acid oxidation is upregulated at the level of gene expression in conjunction with the activation of AMPK (30, 31). MCD mice also displayed evidence of increased fatty acid oxidation, based on their development of ketonemia after a 4-h fast (Table 1). Unlike scd-$1^{-/-}$ mice, however, MCD-fed mice showed no induction of genes controlling fatty acid oxidation (**Fig. 5A**) and no increase in AMPK phosphorylation relative to control mice (Fig. 5B). When palmitate oxidation was measured directly in hepatic

mitochondria from MCD-fed mice, it was 33% higher than that in MCS controls, but the difference did not reach statistical significance (Fig. 5C). CPT-1 activity, also measured in isolated mitochondria, was no different between the two groups of mice (Fig. 5D). Together, these data suggest that the ketonemia observed in MCD-fed mice in vivo results from an increased flux of fatty acids through the β-oxidation pathway rather than from intrinsic upregulation of the oxidative enzymes themselves. The concept of accentuated fatty acid flux through hepatic mitochondria in MCD mice is strengthened by the fact that MCD feeding significantly induced the hepatic expression of uncoupling protein-2 (Fig. 5E). Uncoupling protein-2 induction, in turn, was accompanied by a marked decrease in hepatic ATP levels in MCD-fed mice (1.34 ± 0.02 vs. 0.37 ± 0.01 μmol/g in MCS vs. MCD, respectively; $P < 0.001$).

DISCUSSION

The current study shows that methionine and choline deprivation has pronounced effects on hepatic lipid metabolism that go beyond the inhibition of triglyceride secretion. Specifically, MCD feeding profoundly suppresses SCD-1 gene expression and activity in the liver and to a lesser extent blunts hepatic lipogenesis. Coincident with SCD-1 suppression, MCD feeding causes hypermetabolism, as demonstrated by increased total body energy expenditure, enhanced fatty acid oxidation, and uncoupling of hepatic mitochondria. These derangements are attributable at lease in part to low SCD-1 activity, because mice with targeted disruption of the SCD-1 gene display a similar phenotype (15, 31).

MCD feeding has become popular in recent years as a model of hepatic steatosis and steatohepatitis. The fact that MCD-mediated fatty liver was accompanied by a downregulation of hepatic SCD-1 is unusual, because most other models of fatty liver are characterized by significant induction of this enzyme (32–35). MCD feeding initially induced SCD-1, as would be expected in response to a sucrose-rich diet (36); however, the increase was much less robust and more transient than that in control mice (Fig. 2C). This rapid increase and decline in hepatic SCD-1 mRNA in MCD-fed mice gave the appearance of a negative feedback response. What might be triggering rapid feedback regulation of SCD-1 in this animal model is uncertain, because SCD-1 is not subject to end-product inhibition by monounsaturated fatty acids (37). PUFAs may be responsible, because they can suppress SCD-1 gene expression (37, 38). Our data indicate that PUFAs accumulated disproportionately in the livers of MCD-fed mice compared with MCS controls. A similar disproportionate increase in hepatic PUFAs was noted previously in mice with liver-specific MTP deficiency (12). Both animals experience suppression of SCD-1, which suggests that the inability to mobilize hepatic triglyceride causes unique alterations in hepatic fatty acid composition that significantly affect SCD-1 expression and activity.
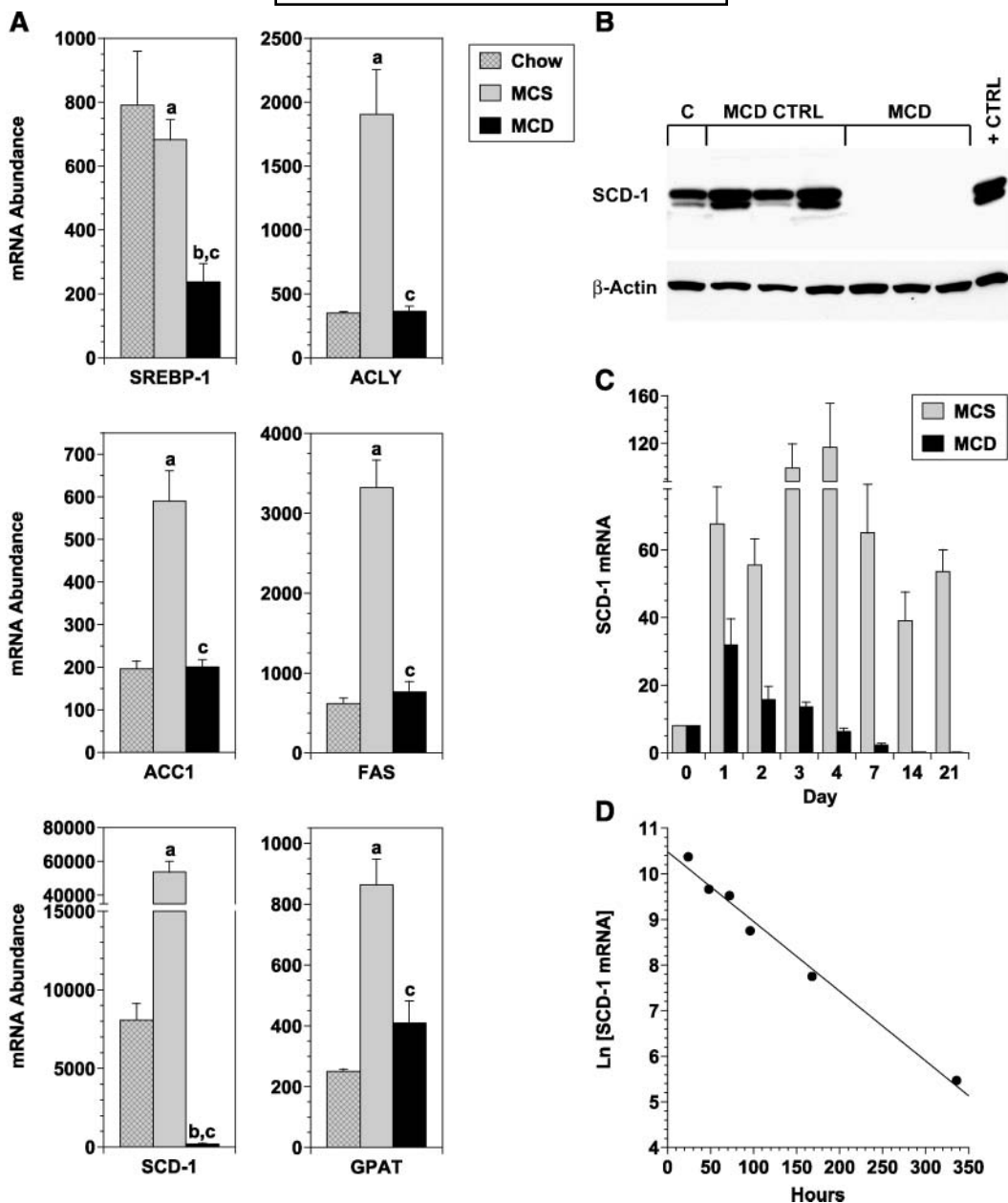
Fig. 2. Changes in hepatic gene and protein expression induced by MCD and control formulas. A: Histograms show the relative abundance of mRNA encoding several lipogenic genes in the livers of mice fed MCD or control formulas for 21 days. mRNA abundance was assessed by quantitative PCR as described in Methods; data were normalized to the expression of mouse β-glucuronidase as an internal control. ACC1, acetyl-coenzyme A carboxylase-1; ACLY, ATP citrate lyase; GPAT, glycerol phosphate acyltransferase; SCD-1, stearoyl-coenzyme A desaturase-1; SREBP-1, sterol-regulatory element binding protein-1. Values represent means ± SEM for n = 5. [a] $P < 0.05$ for MCS versus chow; [b] $P < 0.05$ for MCD versus chow; [c] $P < 0.05$ for MCD versus MCS. B: Immunoblot depicting SCD-1 protein in liver microsomes from mice fed chow (C), the MCS formula, or the MCD formula for 21 days. CTRL, control. C: Histogram depicting the time course of hepatic SCD-1 mRNA regulation in mice fed the MCD or MCS formula. Values represent means ± SEM for n = 5. D: Graph depicting the kinetics of SCD-1 mRNA disappearance in MCD-fed mice from days 1–14.

The decline in SCD-1 expression that occurred in response to MCD feeding was likely a key event in the evolution of other metabolic abnormalities. For example, with the loss of SCD-1 mRNA from the liver, the expression of upstream lipogenic genes was reduced significantly, causing a relative decrease in hepatic lipogenesis well below that expected for mice ingesting a sucrose-rich diet. Downregulation of lipogenic gene expression in MCD-fed mice

could be attributable in part to the MCD-mediated suppression of SREBP-1 mRNA, which regulates a number of target genes involved in the lipogenic pathway; it is important to note, however, that SCD-1 also has significant effects on lipogenic gene expression independent of SREBP-1 (39). Despite profound SCD-1 suppression, MCD-fed mice retained some capacity for hepatic triglyceride synthesis, as shown by their ability to incorporate newly synthesized

TABLE 2. DNL in mice fed MCD and control formulas for 21 days

DNL	Chow	MCS	MCD
Fractional DNL (%)	71.3 ± 1.8	81.8 ± 1.3[a]	34.0 ± 3.8[c,d]
Absolute DNL (mg/liver)	1.4 ± 0.0	14.5 ± 0.3[b]	8.1 ± 0.6[c,d]

DNL, de novo lipogenesis. Mice were fed experimental formulas for a total of 21 days. Three days before the end of the study (day 19), mice were given a loading dose of deuterated saline (30 ml/kg ip) and placed on drinking water containing 8% ^{2}H$_2$O. At the end of the 3 day labeling period, mice were euthanized and livers removed for the measurement of DNL as described in Methods. Fractional DNL represents the proportion of palmitate molecules in the triglyceride fraction that were labeled with deuterium. Absolute DNL represents the total amount of deuterated palmitate present in the liver. Treatment groups were as in Table 1. Values represent means ± SEM for n = 4.

[a] $P < 0.01$ for MCS versus chow.
[b] $P < 0.0001$ for MCS versus chow.
[c] $P < 0.0001$ for MCD versus chow.
[d] $P < 0.0001$ for MCD versus MCS.

Fig. 3. Saturated and monounsaturated fatty acids in the livers of mice fed MCD and control formulas. Histograms depict the absolute amounts of long-chain saturated (C16:0 + C18:0) and monounsaturated (C16:1 + C18:1) fatty acids present in hepatic triglycerides after 21 days on experimental diets. Values represent means ± SEM for n = 5. * $P = 0.002$ for MCD versus MCS.

palmitate into triacylglycerol (Table 2). This is at odds with prior assertions that SCD-1 is essential for triglyceride production (14). It is possible that SCD-1 must be completely absent to block triglyceride synthesis, as in $scd\text{-}1^{-/-}$ mice, whereas in MCD-fed mice, the 2% of SCD-1 mRNA that persisted in the liver was sufficient to support this activity.

SCD-1 suppression in MCD-fed mice was accompanied by hypermetabolism, as it is in $scd\text{-}1^{-/-}$ mice (14, 15). In MCD mice, as in $scd\text{-}1^{-/-}$ mice, hypermetabolism was associated with an increase in fatty acid oxidation in vivo (31). $scd\text{-}1^{-/-}$ mice are believed to upregulate fatty acid β-oxidation to compensate for their reduced ability to channel fatty acids to esterification; in these animals, β-oxidation is induced at the transcriptional level via AMPK (30, 31). In MCD-fed mice, however, fatty acid β-oxidation was enhanced without any evidence of gene induction or
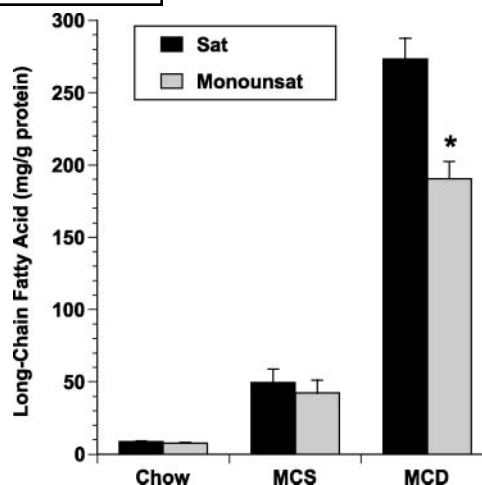
AMPK activation. The failure of MCD feeding to induce the expression of β-oxidation genes despite extremely low levels of SCD-1 may be attributable to the high concentration of fatty acids present in MCD livers. Indeed, recent studies indicate that intracellular fatty acids can interfere with an otherwise strong stimulus to AMPK activation (40) by means of long-chain acyl-CoA ester interference with the phosphorylation of the AMPK kinase complex, LKB1/STRAD/MO25 (41). Because AMPK is not activated in the livers of MCD-fed mice, another mechanism must be responsible for the increase in fatty acid oxidation observed in vivo in response to MCD feeding. Fatty acids are capable

TABLE 3. Fatty acid composition of hepatic triglycerides

	Composition		
Fatty Acid	Chow	MCS	MCD
	% of total		
Myristic, 14:0	1.06 ± 0.08	1.68 ± 0.25	1.38 ± 0.10
Palmitic, 16:0	36.21 ± 1.78	33.98 ± 0.98	25.49 ± 0.70[b,c]
Palmitoleic, 16:1	4.59 ± 0.15	4.67 ± 0.46	1.59 ± 0.11[b,c]
Stearic, 18:0	1.97 ± 0.17	1.66 ± 0.10	4.51 ± 0.17[b,c]
Oleic, 18:1	27.23 ± 1.41	25.18 ± 0.99	19.28 ± 0.39[b,c]
Linoleic, 18:2n6	17.76 ± 1.14	25.94 ± 1.62[a]	29.71 ± 0.68[b]
γ-Linolenic, 18:3n6	0.92 ± 0.26	0.72 ± 0.07	2.46 ± 0.09[b,c]
Eicosenoic, 20:1	1.98 ± 0.20	0.84 ± 0.04[a]	0.73 ± 0.03[b]
Eicosadienoic, 20:2n6	0.90 ± 0.06	0.76 ± 0.06	0.81 ± 0.01
Eicosatrienoic, 20:3n6	0.90 ± 0.09	1.04 ± 0.14	1.93 ± 0.06[b,c]
Arachidonic, 20:4n6	0.91 ± 0.08	1.60 ± 0.25[a]	5.63 ± 0.22[b,c]
Docosatetraenoic, 22:4	0.54 ± 0.11	0.62 ± 0.10	1.80 ± 0.10[b,c]
Docosahexaenoic, 22:6	4.52 ± 0.52	1.32 ± 0.35[a]	4.67 ± 0.36[c]
Total	100.00	100.00	100.00
16:0/16:1	7.9	7.2	15.9
18:0/18:1	0.07	0.07	0.23

Treatment groups were as in Table 1. Values represent means ± SEM for n = 5.
[a] $P < 0.05$ for MCS versus chow.
[b] $P < 0.05$ for MCD versus chow.
[c] $P < 0.05$ for MCD versus MCS.
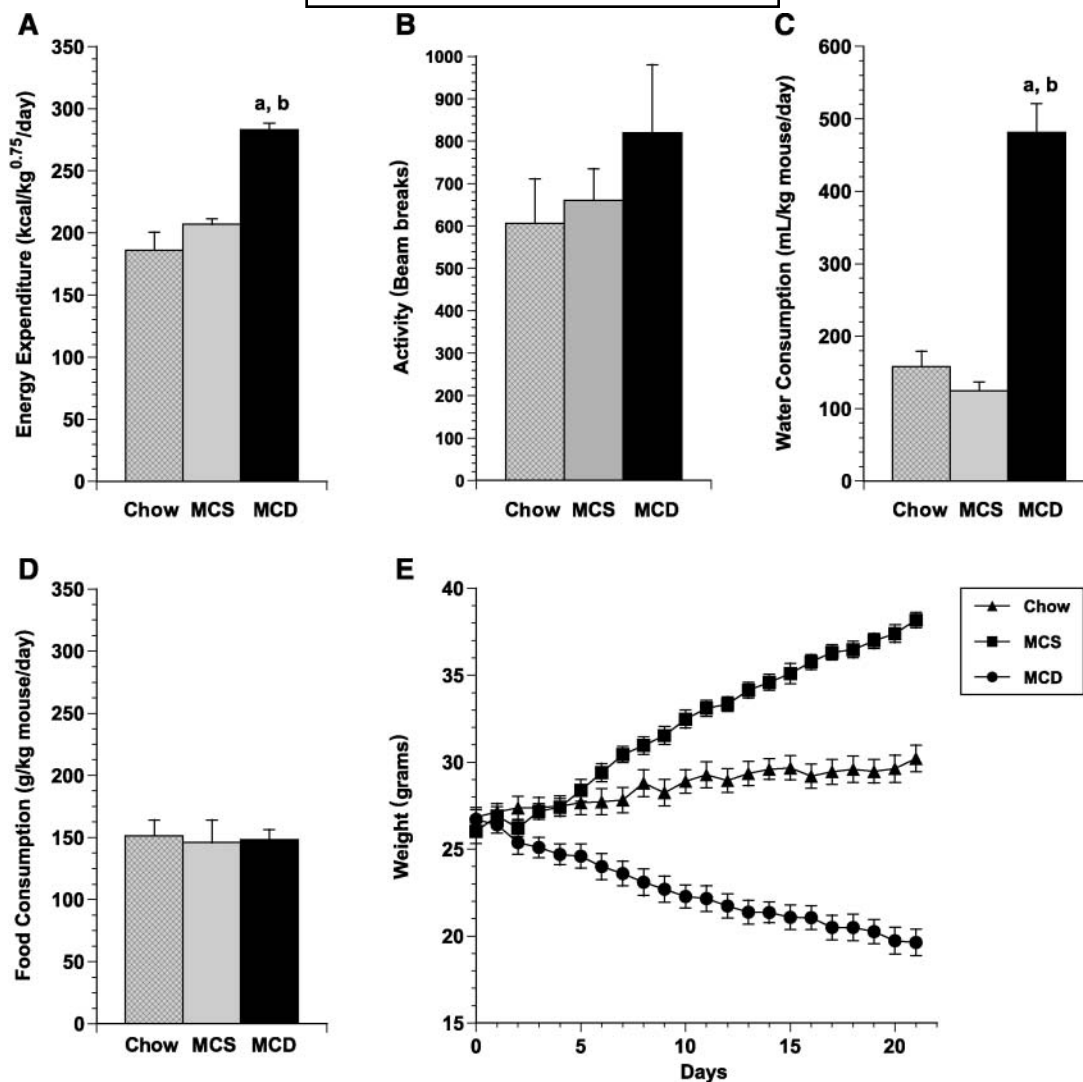
Fig. 4. Energy expenditure, water and food consumption, and body weight in mice fed MCD and control formulas. A–D: Histograms depict energy expenditure (A), physical activity (B), water consumption (C), and food consumption (D) in mice fed chow, MCD, or MCS formulas for 8 days. Measurements were obtained over a 24 h period from day 8 to day 9 on the experimental formulas. Values represent means $\pm$ SEM for n = 9. [a] $P < 0.05$ for MCS versus chow; [b] $P < 0.05$ for MCD versus chow. E: Graph illustrating body weight in mice fed chow, MCS, and MCD formulas for 21 days. Values represent means $\pm$ SEM for n = 5.

of facilitating their own entry into mitochondria by reducing the malonyl-CoA-mediated inhibition of CPT-1 (42). Although at low fatty acid concentrations this appears to occur through AMPK-mediated phosphorylation and inactivation of ACC (43), at higher concentrations fatty acids inhibit ACC directly via allosteric interaction (44). This offers an explanation for why fatty acid flux through the β-oxidation pathway is apparently increased in MCD-fed mice without a significant change in oxidative enzyme expression or enzyme activity in an in vitro assay.

SCD-1-null mice compensate for their hypermetabolic state by significantly increasing their caloric intake. Notably, MCD-fed mice did not increase their food consumption as their energy expenditure increased, and thus they lost a significant amount of weight. This imbalance between energy expenditure and fuel consumption indicates that MCD-fed mice were incorrectly sensing their nutri-

tional status. Several factors were present in MCD mice that should have prompted increased food intake: low circulating lipids, low serum glucose, low insulin levels, and extremely low leptin levels. Why these were ineffective is uncertain, but it is tempting to speculate that fatty acids are again responsible. Circulating long-chain fatty acids curtail food intake by signaling the hypothalamus that the body is in a state of nutritional surplus (45). The accumulation of intracellular long-chain fatty acids within the hypothalamus has a similar effect (46). Although MCD-fed mice do not have increased circulating lipids, they may have high intracellular concentrations of long-chain fatty acids in the brain for the same reason that they do in the liver. Studies are under way to address this question.

Although our data indicate that hypermetabolism in MCD-fed mice is closely linked to the hepatic suppression of SCD-1, these mice began to lose weight before hepatic
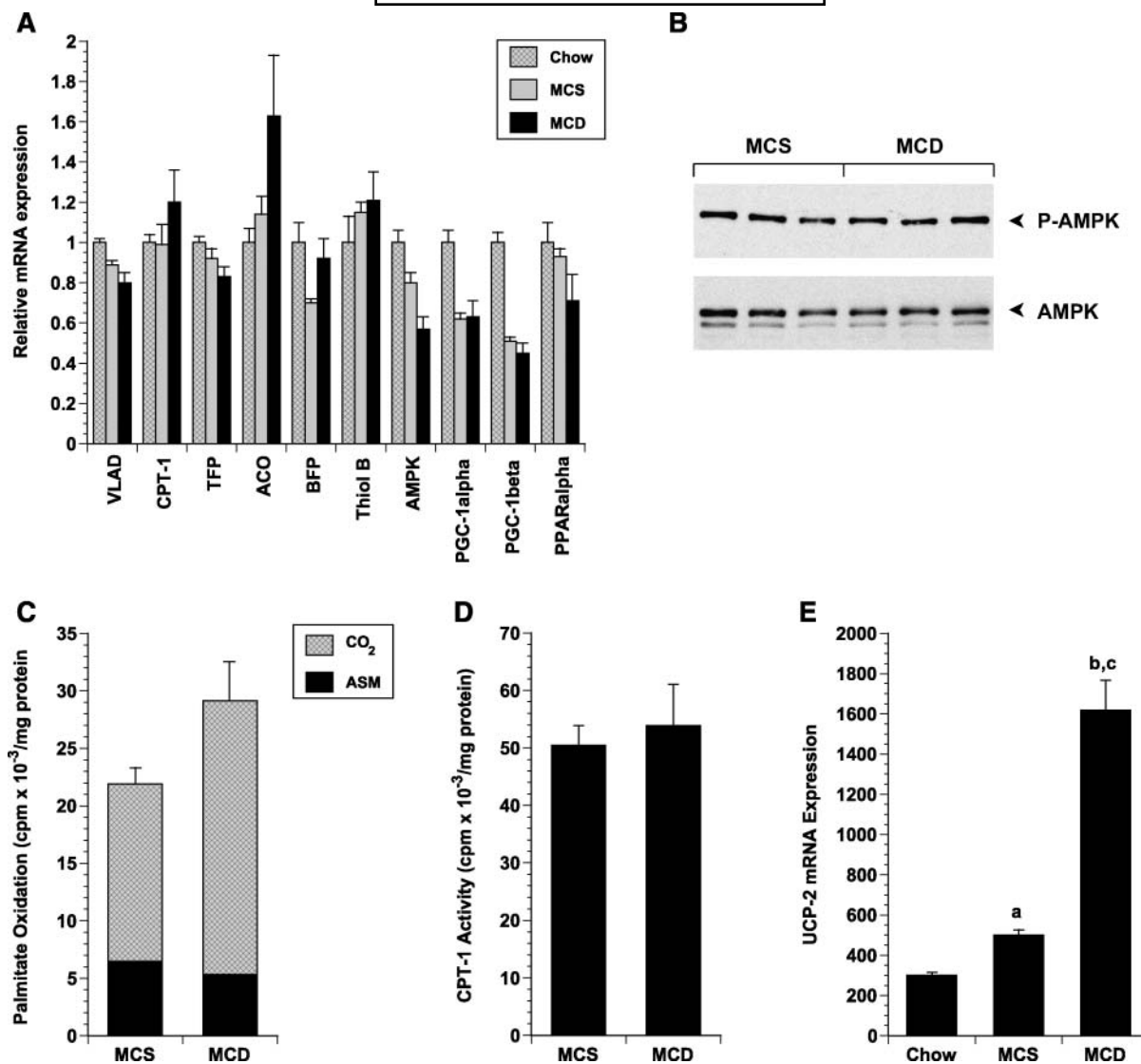
Fig. 5. Fatty acid oxidation in mice fed MCD and control formulas. A: Histogram depicting the relative abundance of genes pertinent to fatty acid oxidation in the livers of chow-, MCS-, or MCD-fed mice. Values represent means ± SEM for n = 5. ACO, acyl-coenzyme A oxidase; AMPK, AMP-activated protein kinase; BFP, bifunctional protein; CPT-1, carnitine palmitoyltransferase-1; PGC-1α/β, peroxisome proliferator-activated receptor-γ coactivator-1α/β; PPARα, peroxisome proliferator-activated receptor α; TFP, trifunctional protein; Thiol B, thiolase B; VLAD, very long chain acyl dehydrogenase. B: Western blot illustrating AMPK and phospho-AMPK (P-AMPK) in the livers of mice fed MCD and MCS formulas for 21 days. C: Histogram showing the conversion of radiolabeled palmitate by hepatic mitochondria isolated from MCS- or MCD-fed mice to acid-soluble intermediates (ASM) and CO_2. Values represent means ± SEM (for total cpm) for n = 6. D: Graph showing CPT-1 activity measured as described in Methods in hepatic mitochondria from MCS- or MCD-fed mice. Values represent means ± SEM for n = 3. E: Histogram demonstrating uncoupling protein-2 (UCP-2) mRNA expression in the livers of mice fed chow, MCS, or MCD formulas for 21 days. Values represent means ± SEM for n = 5. [a] $P < 0.05$ for MCS versus chow; [b] $P < 0.05$ for MCD versus chow; [c] $P < 0.05$ for MCD versus MCS.

SCD-1 mRNA decreased significantly below normal. This suggests that other factors are also at play in the pathogenesis of MCD-mediated weight loss. Liver injury could contribute to weight loss; this is unlikely, however, because MCD-mediated steatohepatitis is completely preventable by drug treatment without any concomitant improvement in weight loss (47). Muscle is an important contributor to total body energy expenditure, particularly during periods of activity (48). MCD feeding probably influences SCD-1 in this tissue as it does in liver, perhaps with even more rapid kinetics. Further exploration of the effect of MCD feeding on extrahepatic organs will be informative.

Noteworthy in our study is that MCD-mediated downregulation of SCD-1 did not alleviate hepatic steatosis. At face value, this appears paradoxical, because SCD-1 suppression markedly improves steatosis in other experimental models of fatty liver (33, 49) and SCD-1 antagonists are under development as treatments for hepatic steatosis and obesity (50, 51). In fatty liver caused by leptin deficiency or lipoatrophy, however, the cellular machinery for exporting hepatic triglyceride is intact. Thus, augmenting hepatic fat disposal by inhibiting SCD-1 significantly reduces the amount of fat retained within the liver. MCD-fed mice, by contrast, have marked impairment of hepatic tri-

glyceride secretion. In these animals, the degree to which SCD-1 suppression facilitated hepatic fat disposal was clearly inadequate to compensate for their defect in triglyceride export. This suggests that humans with hepatic steatosis attributable to impaired hepatic triglyceride secretion, such as those with MTP polymorphisms (52, 53), would not benefit from SCD-1 inhibition.

In summary, inhibiting hepatic triglyceride secretion by feeding mice a diet completely devoid of methionine and choline provokes a profound suppression of SCD-1 in the liver. SCD-1 suppression is likely a compensatory mechanism, designed to reduce lipid synthesis and enhance lipid oxidation under conditions in which triglyceride export is inactive. Because the MCD formula is rich in sucrose, DNL continues despite efforts at downregulation; this exacerbates the hepatic lipid accumulation prompted initially by VLDL secretion blockade. The movement of hepatic fatty acids through the β-oxidation pathway is increased in MCD-fed mice, which in turn increases total body energy expenditure and promotes mitochondrial uncoupling. These changes are not offset by increased food intake, for reasons that are unclear. The net result of these metabolic derangements is a unique form of lipodystrophy, with significant weight loss in combination with hepatic steatosis.∎

REFERENCES

1. Leclercq, I. A., G. C. Farrell, J. Field, D. R. Bell, F. J. Gonzalez, and G. R. Robertson. 2000. CYP2E1 and CYP4A as microsomal catalysts of lipid peroxides in murine nonalcoholic steatohepatitis. *J. Clin. Invest.* **105:** 1067–1075.

2. Yao, Z. M., and D. E. Vance. 1988. The active synthesis of phosphatidylcholine is required for very low density lipoprotein secretion from rat hepatocytes. *J. Biol. Chem.* **263:** 2998–3004.

3. Vance, J. E., and D. E. Vance. 1985. The role of phosphatidylcholine biosynthesis in the secretion of lipoproteins from hepatocytes. *Can. J. Biochem. Cell Biol.* **63:** 870–881.

4. Kulinski, A., D. E. Vance, and J. E. Vance. 2004. A choline-deficient diet in mice inhibits neither the CDP-choline pathway for phosphatidylcholine synthesis in hepatocytes nor apolipoprotein B secretion. *J. Biol. Chem.* **279:** 23916–23924.

5. Weltman, M. D., G. C. Farrell, and C. Liddle. 1996. Increased hepatocyte CYP2E1 expression in a rat nutritional model of hepatic steatosis with inflammation. *Gastroenterology.* **111:** 1645–1653.

6. Ip, E., G. C. Farrell, P. Hall, G. Robertson, and I. Leclercq. 2004. Administration of the potent PPARalpha agonist, Wy-14,643, reverses nutritional fibrosis and steatohepatitis in mice. *Hepatology.* **39:** 1286–1296.

7. Costet, P., C. Legendre, J. More, A. Edgar, P. Galtier, and T. Pineau. 1998. Peroxisome proliferator-activated receptor alpha-isoform deficiency leads to progressive dyslipidemia with sexually dimorphic obesity and steatosis. *J. Biol. Chem.* **273:** 29577–29585.

8. Moitra, J., M. M. Mason, M. Olive, D. Krylov, O. Gavrilova, B. Marcus-Samuels, L. Feigenbaum, E. Lee, T. Aoyama, M. Eckhaus, et al. 1998. Life without white fat: a transgenic mouse. *Genes Dev.* **12:** 3168–3181.

9. Shimomura, I., Y. Bashmakov, and J. D. Horton. 1999. Increased levels of nuclear SREBP-1c associated with fatty livers in two mouse models of diabetes mellitus. *J. Biol. Chem.* **274:** 30028–30032.

10. Baffy, G., C. Y. Zhang, J. N. Glickman, and B. B. Lowell. 2002. Obesity-related fatty liver is unchanged in mice deficient for mitochondrial uncoupling protein 2. *Hepatology.* **35:** 753–761.

11. Raabe, M., M. M. Veniant, M. A. Sullivan, C. H. Zlot, J. Bjorkegren, L. B. Nielsen, J. S. Wong, R. L. Hamilton, and S. G. Young. 1999. Analysis of the role of microsomal triglyceride transfer protein in the liver of tissue-specific knockout mice. *J. Clin. Invest.* **103:** 1287–1298.

12. Bjorkegren, J., A. Beigneux, M. O. Bergo, J. J. Maher, and S. G. Young. 2002. Blocking the secretion of hepatic very low density lipoproteins renders the liver more susceptible to toxin-induced injury. *J. Biol. Chem.* **277:** 5476–5483.

13. Ntambi, J. M., and M. Miyazaki. 2004. Regulation of stearoyl-CoA desaturases and role in metabolism. *Prog. Lipid Res.* **43:** 91–104.

14. Miyazaki, M., Y. C. Kim, and J. M. Ntambi. 2001. A lipogenic diet in mice with a disruption of the stearoyl-CoA desaturase 1 gene reveals a stringent requirement of endogenous monounsaturated fatty acids for triglyceride synthesis. *J. Lipid Res.* **42:** 1018–1024.

15. Ntambi, J. M., M. Miyazaki, J. P. Stoehr, H. Lan, C. M. Kendziorski, B. S. Yandell, Y. Song, P. Cohen, J. M. Friedman, and A. D. Attie. 2002. Loss of stearoyl-CoA desaturase-1 function protects mice against adiposity. *Proc. Natl. Acad. Sci. USA.* **99:** 11482–11486.

16. Ginzinger, D. G. 2002. Gene quantification using real-time quantitative PCR: an emerging technology hits the mainstream. *Exp. Hematol.* **30:** 503–512.

17. Livak, K. J., and T. D. Schmittgen. 2001. Analysis of relative gene expression data using real-time quantitative PCR and the 2(-Delta Delta C(T)) method. *Methods.* **25:** 402–408.

18. Watkins, S. M., P. R. Reifsnyder, H. J. Pan, J. B. German, and E. H. Leiter. 2002. Lipid metabolome-wide effects of the PPARgamma agonist rosiglitazone. *J. Lipid Res.* **43:** 1809–1817.

19. Ozols, J. 1997. Degradation of hepatic stearyl CoA delta 9-desaturase. *Mol. Biol. Cell.* **8:** 2281–2290.

20. Hellerstein, M. K., and R. A. Neese. 1999. Mass isotopomer distribution analysis at eight years: theoretical, analytic, and experimental considerations. *Am. J. Physiol.* **276:** E1146–E1170.

21. Hellerstein, M. K., C. Kletke, S. Kaempfer, K. Wu, and C. H. Shackleton. 1991. Use of mass isotopomer distributions in secreted lipids to sample lipogenic acetyl-CoA pool in vivo in humans. *Am. J. Physiol.* **261:** E479–E486.

22. Hellerstein, M. K., M. Christiansen, S. Kaempfer, C. Kletke, K. Wu, J. S. Reid, K. Mulligan, N. S. Hellerstein, and C. H. Shackleton. 1991. Measurement of de novo hepatic lipogenesis in humans using stable isotopes. *J. Clin. Invest.* **87:** 1841–1852.

23. Jung, H. R., S. M. Turner, R. A. Neese, S. G. Young, and M. K. Hellerstein. 1999. Metabolic adaptations to dietary fat malabsorption in chylomicron-deficient mice. *Biochem. J.* **343:** 473–478.

24. Jones, P. J. 1996. Tracing lipogenesis in humans using deuterated water. *Can. J. Physiol. Pharmacol.* **74:** 755–760.

25. Lee, W. N., S. Bassilian, H. O. Ajie, D. A. Schoeller, J. Edmond, E. A. Bergner, and L. O. Byerley. 1994. In vivo measurement of fatty acids and cholesterol synthesis using D₂O and mass isotopomer analysis. *Am. J. Physiol.* **266:** E699–E708.

26. McGarry, J. D., S. E. Mills, C. S. Long, and D. W. Foster. 1983. Observations on the affinity for carnitine, and malonyl-CoA sensitivity, of carnitine palmitoyltransferase I in animal and human tissues. Demonstration of the presence of malonyl-CoA in non-hepatic tissues of the rat. *Biochem. J.* **214:** 21–28.

27. Esser, V., N. F. Brown, A. T. Cowan, D. W. Foster, and J. D. McGarry. 1996. Expression of a cDNA isolated from rat brown adipose tissue and heart identifies the product as the muscle isoform of carnitine palmitoyltransferase I (M-CPT I). M-CPT I is the predominant CPT I isoform expressed in both white (epididymal) and brown adipocytes. *J. Biol. Chem.* **271:** 6972–6977.

28. Gavrilova, O., L. R. Leon, B. Marcus-Samuels, M. M. Mason, A. L. Castle, S. Refetoff, C. Vinson, and M. L. Reitman. 1999. Torpor in mice is induced by both leptin-dependent and -independent mechanisms. *Proc. Natl. Acad. Sci. USA.* **96:** 14623–14628.

29. Shimomura, I., R. E. Hammer, J. A. Richardson, S. Ikemoto, Y. Bashmakov, J. L. Goldstein, and M. S. Brown. 1998. Insulin resistance and diabetes mellitus in transgenic mice expressing nuclear SREBP-1c in adipose tissue: model for congenital generalized lipodystrophy. *Genes Dev.* **12:** 3182–3194.

30. Miyazaki, M., A. Dobrzyn, H. Sampath, S. H. Lee, W. C. Man, K. Chu, J. M. Peters, F. J. Gonzalez, and J. M. Ntambi. 2004. Reduced adiposity and liver steatosis by stearoyl-CoA desaturase deficiency are independent of peroxisome proliferator-activated receptor-alpha. *J. Biol. Chem.* **279:** 35017–35024.

31. Dobrzyn, P., A. Dobrzyn, M. Miyazaki, P. Cohen, E. Asilmaz, D. G. Hardie, J. M. Friedman, and J. M. Ntambi. 2004. Stearoyl-CoA desaturase 1 deficiency increases fatty acid oxidation by activating AMP-activated protein kinase in liver. *Proc. Natl. Acad. Sci. USA.* **101:** 6409–6414.

32. Enser, M. 1975. Desaturation of stearic acid by liver and adipose tissue from obese-hyperglycaemic mice (ob/ob). *Biochem. J.* **148:** 551–555.

33. Cohen, P., M. Miyazaki, N. D. Socci, A. Hagge-Greenberg, W. Liedtke, A. A. Soukas, R. Sharma, L. C. Hudgins, J. M. Ntambi, and J. M. Friedman. 2002. Role for stearoyl-CoA desaturase-1 in leptin-mediated weight loss. *Science.* **297:** 240–243.

34. Lopez, I. P., A. Marti, F. I. Milagro, M. J. Zulet Md Mde, M. J. Moreno-Aliaga, J. A. Martinez, and C. De Miguel. 2003. DNA microarray analysis of genes differentially expressed in diet-induced (cafeteria) obese rats. *Obes. Res.* **11:** 188–194.

35. Tomita, K., T. Azuma, N. Kitamura, J. Nishida, G. Tamiya, A. Oka, S. Inokuchi, T. Nishimura, M. Suematsu, and H. Ishii. 2004. Pioglitazone prevents alcohol-induced fatty liver in rats through up-regulation of c-Met. *Gastroenterology.* **126:** 873–885.

36. Worcester, N. A., K. R. Bruckdorfer, T. Hallinan, A. J. Wilkins, J. A. Mann, and J. Yudkins. 1979. The influence of diet and diabetes on stearoyl coenzyme A desaturase (EC 1.14.99.5) activity and fatty acid composition in rat tissues. *Br. J. Nutr.* **41:** 239–252.

37. Sessler, A. M., N. Kaur, J. P. Palta, and J. M. Ntambi. 1996. Regulation of stearoyl-CoA desaturase 1 mRNA stability by polyunsaturated fatty acids in 3T3-L1 adipocytes. *J. Biol. Chem.* **271:** 29854–29858.

38. Ntambi, J. M. 1992. Dietary regulation of stearoyl-CoA desaturase 1 gene expression in mouse liver. *J. Biol. Chem.* **267:** 10925–10930.

39. Miyazaki, M., A. Dobrzyn, W. C. Man, K. Chu, H. Sampath, H. J. Kim, and J. M. Ntambi. 2004. Stearoyl-CoA desaturase 1 gene expression is necessary for fructose-mediated induction of lipogenic gene expression by sterol regulatory element-binding protein-1c-dependent and -independent mechanisms. *J. Biol. Chem.* **279:** 25164–25171.

40. Tanaka, T., S. Hidaka, H. Masuzaki, S. Yasue, Y. Minokoshi, K. Ebihara, H. Chusho, Y. Ogawa, T. Toyoda, K. Sato, et al. 2005. Skeletal muscle AMP-activated protein kinase phosphorylation par-

41. Taylor, E. B., W. J. Ellingson, J. D. Lamb, D. G. Chesser, and W. W. Winder. 2005. Long-chain acyl-CoA esters inhibit phosphorylation of AMP-activated protein kinase at threonine-172 by LKB1/STRAD/MO25. *Am. J. Physiol. Endocrinol. Metab.* **288:** E1055–E1061.

42. Merrill, G. F., E. J. Kurth, B. B. Rasmussen, and W. W. Winder. 1998. Influence of malonyl-CoA and palmitate concentration on rate of palmitate oxidation in rat muscle. *J. Appl. Physiol.* **85:** 1909–1914.

43. Fediuc, S., M. P. Gaidhu, and R. B. Ceddia. 2005. Regulation of AMP-activated protein kinase and acetyl-CoA carboxylase phosphorylation by palmitate in skeletal muscle cells. *J. Lipid Res.* **47:** 412–420.

44. Trumble, G. E., M. A. Smith, and W. W. Winder. 1995. Purification and characterization of rat skeletal muscle acetyl-CoA carboxylase. *Eur. J. Biochem.* **231:** 192–198.

45. Lam, T. K., G. J. Schwartz, and L. Rossetti. 2005. Hypothalamic sensing of fatty acids. *Nat. Neurosci.* **8:** 579–584.

46. Obici, S., Z. Feng, A. Arduini, R. Conti, and L. Rossetti. 2003. Inhibition of hypothalamic carnitine palmitoyltransferase-1 decreases food intake and glucose production. *Nat. Med.* **9:** 756–761.

47. Ip, E., G. C. Farrell, G. R. Robertson, P. Hall, R. Kirsch, and I. A. Leclercq. 2003. Central role of PPARalpha-dependent hepatic lipid turnover in dietary steatohepatitis in mice. *Hepatology.* **38:** 123–132.

48. Gallagher, D., D. Belmonte, P. Deurenberg, Z. Wang, N. Krasnow, F. X. Pi-Sunyer, and S. B. Heymsfield. 1998. Organ-tissue mass measurement allows modeling of REE and metabolically active tissue mass. *Am. J. Physiol.* **275:** E249–E258.

49. Asilmaz, E., P. Cohen, M. Miyazaki, P. Dobrzyn, K. Ueki, G. Fayzikhodjaeva, A. A. Soukas, C. R. Kahn, J. M. Ntambi, N. D. Socci, et al. 2004. Site and mechanism of leptin action in a rodent form of congenital lipodystrophy. *J. Clin. Invest.* **113:** 414–424.

50. Dobrzyn, A., and J. M. Ntambi. 2005. Stearoyl-CoA desaturase as a new drug target for obesity treatment. *Obes. Rev.* **6:** 169–174.

51. Jiang, G., Z. Li, F. Liu, K. Ellsworth, Q. Dallas-Yang, M. Wu, J. Ronan, C. Esau, C. Murphy, D. Szalkowski, et al. 2005. Prevention of obesity in mice by antisense oligonucleotide inhibitors of stearoyl-CoA desaturase-1. *J. Clin. Invest.* **115:** 1030–1038.

52. Bernard, S., S. Touzet, I. Personne, V. Lapras, P. J. Bondon, F. Berthezene, and P. Moulin. 2000. Association between microsomal triglyceride transfer protein gene polymorphism and the biological features of liver steatosis in patients with type II diabetes. *Diabetologia.* **43:** 995–999.

53. Namikawa, C., Z. Shu-Ping, J. R. Vyselaar, Y. Nozaki, Y. Nemoto, M. Ono, N. Akisawa, T. Saibara, M. Hiroi, H. Enzan, et al. 2004. Polymorphisms of microsomal triglyceride transfer protein gene and manganese superoxide dismutase gene in non-alcoholic steatohepatitis. *J. Hepatol.* **40:** 781–786.